ACS Catalysis

Research Article

Cite This: ACS Catal. 2018, 8, 3194−3201

pubs.acs.org/acscatalysis

# Incorporation of Imidazolium-Based Poly(ionic liquid)s into a Metal−Organic Framework for $CO_2$ Capture and Conversion

Meili Ding and Hai-Long Jiang*

Hefei National Laboratory for Physical Sciences at the Microscale, CAS Key Laboratory of Soft Matter Chemistry, Collaborative Innovation Center of Suzhou Nano Science and Technology, School of Chemistry and Materials Science, University of Science and Technology of China, Hefei, Anhui 230026, P. R. China

Supporting Information

**ABSTRACT:** The rational integration of multiple functional components into a composite material could result in enhanced activity tailored for specific applications. Herein, imidazolium-based poly(ionic liquid)s (denoted as polyILs) have been confined into the metal−organic framework (MOF) material MIL-101 via *in situ* polymerization of encapsulated monomers. The resultant composite polyILs@MIL-101 exhibits good $CO_2$ capture capability that is beneficial for the catalysis of the cycloaddition of $CO_2$ with epoxides to form cyclic carbonates at subatmospheric pressure in the absence of any cocatalyst. The significantly enhanced activity of polyILs@MIL-101, compared to either MIL-101 or polyILs, is attributed to the synergistic effect among the good $CO_2$ enrichment capacity, the Lewis acid sites in the MOF, as well as the Lewis base sites in the polyILs.

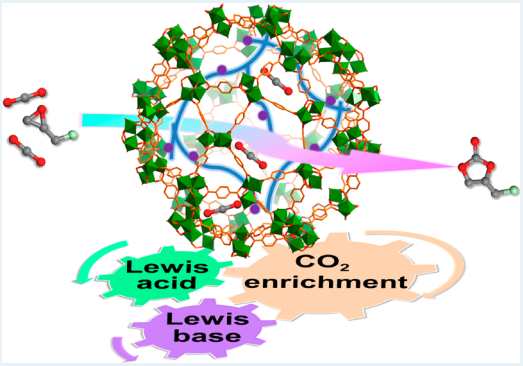


**KEYWORDS:** *metal−organic framework, ionic liquid, heterogeneous catalysis, carbon dioxide fixation, cyclic carbonate*

## 1. INTRODUCTION

Anthropogenic emission of greenhouse gases, the main component of which is carbon dioxide ($CO_2$), has been considered to cause global warming and ocean acidification.[1,2] Despite its undesirable effects, $CO_2$ is indeed an inexpensive, abundant, renewable, and nontoxic C1 resource, which can be fixated into diverse value-added chemical feedstocks.[3−7] Among all $CO_2$ fixation strategies, the cycloaddition of epoxides with $CO_2$ to form cyclic carbonates is one of the most promising, owing to the high atomic economy, green reaction, and the versatile structures of cyclic carbonates, which can be further transformed into diverse fine chemicals.[5,7] A variety of homogeneous and heterogeneous catalysts have been developed for the coupling of $CO_2$ and epoxides.[5,7−14] In general, homogeneous catalysts have higher efficiency but are harder to isolate from the reaction systems. On the other hand, heterogeneous catalysts are less efficient but are easier to be isolated and recycled. Ionic liquids (ILs), a kind of environment-friendly solvent with low vapor pressure, good solubility, high stability, and tunable acidity, were found to possess excellent catalytic activity in the $CO_2$ fixation reaction.[15−18] However, ILs also have some disadvantages, including the complicated process of catalyst recovery from the reaction system, high viscosity, and relatively low efficiency of utilization as solvents or catalysts,[19−23] which severely hamper their industrial application. To overcome these challenges, ILs are commonly supported or immobilized to different materials (e.g., silica, metal oxides, and polymers) to obtain heterogeneous catalysts for the $CO_2$ cycloaddition reaction.[20−23] Unfortunately, the type of grafted ILs is seriously limited to some solid supports due to the requirement for special groups, such as the hydroxyl group on the surface of $SiO_2$.[20−23] Moreover, many IL-based catalysts require harsh reaction conditions (high temperature/pressure) because of the lack of multiple active sites (e.g., acid and base sites) to synergistically promote the reaction.[22−24] It remains challenging to develop an IL-based heterogeneous catalyst, which is efficient for the $CO_2$ cycloaddition reaction in the absence of a cocatalyst, under mild temperature and subatmospheric pressure of $CO_2$.

We consider that the above challenges might be solved by immobilizing ILs into porous materials with high surface areas and particular active sites. The porous structure and high surface area will ensure accessibility of ILs and good $CO_2$ adsorption, and multiple active sites from both components can be synergized, thus improving the catalytic efficiency. Toward this end, we chose metal−organic frameworks (MOFs), a class of porous crystalline materials featuring rich structural diversity and tailorability, selective $CO_2$ adsorption power, high surface areas,[24−27] and the presence of acidic or basic sites capable of activating either epoxides or $CO_2$ molecules.[5,7] Nevertheless, the simple incorporation of ILs into MOFs was found to suffer from the strong interaction of both components, which led to the lack of intrinsic characters of ILs and/or the occupation of active sites in MOFs, which are detrimental to the activity of

Received: October 6, 2017
Revised: March 4, 2018
Published: March 8, 2018






DOI: 10.1021/acscatal.7b03404
ACS Catal. 2018, 8, 3194−3201

Scheme 1. Schematic Illustration Showing the Preparation of polyILs@MIL-101

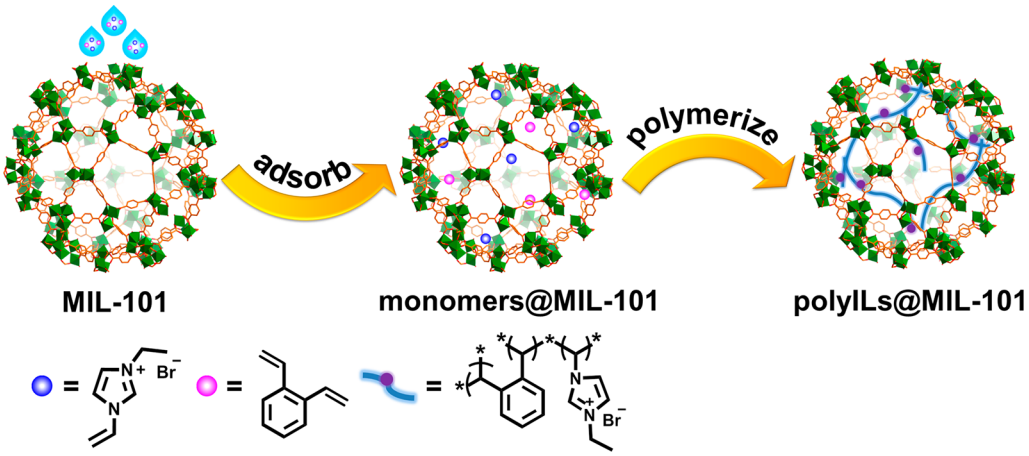


the ILs@MOF composites.[28−30] To circumvent this issue, ILs have been successfully bound to the organic linkers of MOFs, either prior to or after the MOF synthesis.[31−34] These strategies however often require complicated catalyst preparation processes and/or special active groups (e.g., $-NH_2$) at the linkers for postsynthetic modification. Therefore, it still remains a huge challenge to develop a facile and universal approach to fabricate IL-MOF composites by integrating their respective merits for efficient $CO_2$ conversion.

We envision that *in situ* polymerization of ILs inside MOF pores could result in stable heterogeneous composites, in which the intrinsic properties of both components can be retained well for the $CO_2$ fixation reaction. Along this line, 1-vinyl-3-ethylimidazolium bromide (VEIMBr) and the cross-linker of *ortho*-divinylbenzene (o-DVB) were collectively introduced into a MOF and then copolymerized to give the composite of imidazolium-based poly(ionic liquid)s (polyILs) threading in the MOF, MIL-101, denoted as polyILs@MIL-101 (Scheme 1). The MOF porous structure was largely retained in the composite, facilitating the transport of catalytic substrates/products and $CO_2$ sorption. We were delighted to find that the exposed Lewis acid sites in the MOF and the Lewis base sites ($Br^-$) from polyILs synergistically promote the activation and subsequent reaction of $CO_2$ and epoxides. As a result, the composite catalyst exhibits excellent catalytic activity and recyclability toward $CO_2$ cycloaddition with epoxides under mild conditions (1 bar or lower $CO_2$ pressure, ≤70 °C). It is noteworthy that our catalytic system does not require any cocatalysts, and the catalytic activity almost remains even at relatively low pressures of $CO_2$, thanks to the high $CO_2$ capture capability of the composite, affording direct evidence on the positive correlation between $CO_2$ capture and conversion. In addition, we would point out that the polymerized IL@MOF composites have been recently constructed for alkaline anion exchange membranes.[35] By contrast, our work employs a different IL to afford a new bulk composite and reports the first trial of such polyILs-MOF material for $CO_2$ cycloaddition reaction.

## 2. EXPERIMENTAL SECTION

**2.1. Material and Instrumentation.** All chemicals were purchased from commercial sources and used without further treatment. Deionized water, with the specific resistance of 18.25 MΩ cm, was acquired by reverse osmosis, followed by ion-exchange and filtration (Cleaned Water Treatment Co., Ltd., Hefei). The powder X-ray diffraction patterns (XRD) were recorded on a Japan Rigaku SmartLab rotation anode X-ray diffractometer or a Holland X'Pert PRO fixed anode X-ray diffractometer, equipped with graphite monochromatized Cu K$\alpha$ radiation ($\lambda$ = 1.54 Å). The $N_2$ and $CO_2$ sorption isotherms were measured by an automatic volumetric adsorption equipment (Micrometritics ASAP 2020). The Fourier transform infrared (FT-IR) spectra were collected on a SHIMADZU IR Affinity-1 spectrometer, with KBr discs in the range of 4000 to 400 $cm^{-1}$. The CPMAS $^{13}C$ NMR measurements were carried out with a Bruker AVANCE AV III 400WB spectrometer operating at 100 MHz. Thermogravimetric analysis (TGA) was carried out on a Shimadzu DTG-60H thermogravimetric analyzer, at a ramp rate of 10 °C/min in nitrogen atmosphere. The X-ray photoelectron spectroscopy (XPS) measurements were conducted using an ESCALAB 250Xi high-performance electron spectrometer, using monochromatized Al K$\alpha$ ($h\nu$ = 1486.7 eV) as the excitation source. The contents of C, H, and N were quantified by using a VarioELIII Elemental analyzer. The contents of $Cr^{3+}$ in different catalysts were measured by an Optima 7300 DV inductively coupled plasma atomic emission spectrometer (ICP-AES). The conversion and yield were determined by using a Shimadzu gas chromatograph (GC-2010 Plus with a 0.25 mm × 30 m Rtx-5 capillary column), with an FID detector and high purity nitrogen as the carrier gas. The transmission electron microscopy (TEM) and elemental mapping were acquired on JEOL-2010 and JEOL-2100F, with an electron acceleration energy of 200 kV. To prepare the ultramicrotomed polyILs@MIL-101, the powder was immersed into epoxy resin, and the resin was polymerized at 60 °C for 48 h. Then, the resin block was cut into slices with an ultramicrotome (ULTRACUTE). Finally, thin specimens were collected on a 200 mesh copper grid via the usual drying method for further elemental mapping characterization. The diffuse reflectance infrared Fourier transform (DRIFT) spectra of $CO_2$ adsorption on the sample were collected on a Nicolet iS10 spectrometer with an MCT detector. Before characterization, the sample was activated at 160 °C for 12 h. After that, the sample powder was loaded into the IR reflectance cell and purged by flowing argon (Ar; 20 mL/min) for 20 min at room temperature. Afterward, the spectra of $CO_2$ adsorption were collected under a $CO_2$ flow of ∼3 mL/min until reaching saturated adsorption, and then the weakly adsorbed $CO_2$ was removed under an Ar flow of ∼5 mL/min. The acidity of the catalyst was determined by



DOI: 10.1021/acscatal.7b03404
ACS Catal. 2018, 8, 3194−3201

temperature-programmed desorption of ammonia ($NH_3$-TPD), by using a DAS-7000 Multifunctional automatic adsorption instrument. Before $NH_3$ adsorption, the sample was activated at 150 °C for 4 h in $N_2$ atmosphere. After adsorption of $NH_3$ at 50 °C for 0.5 h, the desorption step was performed from 50 to 400 °C at a heating rate of 10 °C/min. Water contact angle measurements were performed on OCA 40 optical contact angle meter under ambient conditions.

**2.2. Preparation of Samples.** *2.2.1. Preparation of 1-Vinyl-3-ethylimidazolium Bromide (VEIMBr).* The 1-vinyl-3-ethylimidazolium bromide was prepared according to the previous literature with a few modifications.[36] Typically, a mixture of bromoethane (4 g, 36.7 mmol) and 1-vinylimidazole (2 g, 21.3 mmol) was added to a 25 mL two-necked round-bottom flask under a nitrogen atmosphere and then heated to 70 °C for 16 h. After cooling to room temperature, the resulting white solid was obtained by washing with ethyl acetate three times and drying overnight at 60 °C in vacuum. $^1$H NMR (400 MHz, $CDCl_3$): $\delta$ (ppm) 10.20 (s, 1H), 8.25 (t, 1H), 8.02 (s, 2H), 7.53 (dd, 1H), 6.17 (dd, 1H), 5.47 (dd, 1H), 4.53 (q, 2H), 1.64 (t, 3H).

*2.2.2. Preparation of MIL-101.* MIL-101 was synthesized based on the previous literature with minor modifications.[37] Typically, a mixture of terephthalic acid (1.8 g, 10.8 mmol), $Cr(NO_3)_3{\cdot}9H_2O$ (4.33 g, 10.8 mmol), and HF (0.3 mL, 1.5 mmol) was dispersed in water (52 mL) and then reacted at 200 °C for 8 h. The as-synthesized MIL-101 was refluxed in water for 24 h, followed by refluxing in ethanol for 24 h twice, in $NH_4F$ aqueous solution at 85 °C for 12 h, and then washed with hot ethanol to eliminate the unreacted BDC trapped in the pores of MIL-101. The resultant green solid was finally dried overnight at 160 °C under vacuum for further use.

*2.2.3. Preparation of Bulk polyILs.* A mixture of VEIMBr (100 mg, 0.5 mmol), o-DVB (60 $\mu$L, 0.42 mmol), AIBN (3 mg, 0.02 mmol), and ethanol (300 $\mu$L) was added into a 10 mL round-bottom flask successively and then heated to 70 °C for 24 h under nitrogen protection. After that, the white precipitates were collected, washed with ethanol and methanol several times, and dried overnight at 60 °C in vacuum.

*2.2.4. Preparation of polyILs@MIL-101.* Typically, activated MIL-101 (200 mg) was mixed and gently grinded with a mixture of VEIMBr (100 mg, 0.5 mmol), o-DVB (60 $\mu$L, 0.42 mmol), AIBN (3 mg, 0.02 mmol), and ethanol (300 $\mu$L) in a mortar until visually dry. Afterward, the mixture was sealed in a 10 mL round-bottom flask and heated to 70 °C for 24 h under nitrogen protection. Finally, the resultant product was collected, washed with ethanol and methanol several times, and dried overnight at 60 °C in vacuum.

*2.2.5. Preparation of PVEIMBr@MIL-101.* PVEIMBr@MIL-101 was prepared by a similar procedure to that of polyILs@MIL-101, except for the absence of o-DVB.

**2.3. Catalytic Activity Evaluation.** *2.3.1. Cycloaddition of $CO_2$ and Epoxide.* Typically, a mixture of polyILs@MIL-101 (100 mg), epoxide (1 mmol), and acetonitrile (2 mL) was added into a 5 mL round-bottom flask, which was connected to a $CO_2$ balloon. Then, the mixture was stirred at 70 °C for 24 h. Note that the amount of other catalysts, including VEIMBr, bulk polyILs, and MIL-101, was calculated based on the fixed N or $Cr^{3+}$ content (evaluated by elemental analysis and ICP results) in polyILs@MIL-101 (Table S1). For the reaction under low $CO_2$ pressures, the same procedure as above was employed, except for using a mixed $CO_2/N_2$ gas and *N*,*N*-dimethylformamide as the C1 source and solvent, respectively. For the reaction under 1.50 bar $CO_2$, the catalytic reaction was conducted in a 10 mL Teflon-lined stainless-steel autoclave. Then, the same procedure as above was performed, except for using 1.50 bar $CO_2$ as the C1 source.

*2.3.2. Recyclability Investigation for polyILs@MIL-101 Catalyst.* After the cycloaddition reaction of $CO_2$ and epichlorohydrin for 24 h, the composite catalyst was separated by centrifugation, washed with methanol several times, and dried overnight at 60 °C in vacuum. After that, the catalyst was used for the subsequent cycle of $CO_2$ cycloaddition with epichlorohydrin. The same procedure was conducted ten times to examine the recyclability of polyILs@MIL-101.

**2.4. Detection of Bromide Ion.** As-synthesized polyILs@MIL-101 (6 mg) was immersed in water (4 mL), and the mixture was sonicated for 20 min by using a commercial ultrasonic cleaner. After that, the filtrate was obtained by simple filtration. Then, the $AgNO_3$ solution (0.05 mM) was added dropwise to the above filtrate and the VEIMBr aqueous solution, respectively.

**2.5. Digestion of MIL-101 and polyILs@MIL-101.** To prepare samples for the IR, ICP, and NMR tests, as well as the evaluation of the polyILs loading in polyILs@MIL-101, both MIL-101 and polyILs@MIL-101 (40 mg) were completely digested by the NaOH aqueous solution (4 M, 4 mL). The insoluble polymer (polyILs) was collected by centrifugation, washing with water and methanol for several times, and drying overnight at 60 °C in vacuum. On the other hand, the pH of the soluble solution (after digestion) was adjusted by hydrochloric acid to be lower than 7, and the system was purified by removing terephthalic acid before the ICP measurements.

## 3. RESULTS AND DISCUSSION

A representative mesoporous MOF, MIL-101 with the formula $Cr_3X(H_2O)_2O(BDC)_3{\cdot}nH_2O$ (BDC = benzene-1,4-dicarboxylate, X = F or OH, $n \approx 25$),[37] was employed owing to its intersecting 3D structure, high physicochemical stability, high surface area ($S_{BET}$ = ~4100 $m^2/g$), and large pore sizes (~3 nm) that are desirable to encapsulate the polyILs. Moreover, upon activation by simple heating, MIL-101 is able to afford exposed Cr(III) centers, serving as Lewis acid sites for catalysis.

The monomers VEIMBr and o-DVB were introduced into the MOF pores by grinding the MIL-101 powder in an ethanol solution containing the two monomers, and radical copolymerization was initiated by 2,2′-azobis(isobutyronitrile) (AIBN) at a moderate temperature (70 °C) to give polyILs@MIL-101 (see section 2) with 26 wt % loading of polyILs (Table S2). In order to examine whether all of the unreacted VEIMBr was completely removed from the MOF pores, detection of bromide ion was performed by adding $AgNO_3$ into the filtrate obtained by ultrasonic cleaning of polyILs@MIL-101 (see section 2). In contrast to the formation of a very pale creamy precipitate in VEIMBr solution after adding the $AgNO_3$ solution, no obvious change was observed in the filtrate from polyILs@MIL-101 (Figure S1), revealing almost no residual unreacted VEIMBr in polyILs@MIL-101. To demonstrate whether the polymerization of two monomers in MIL-101 took place, bulk polyILs were synthesized under similar conditions in the absence of MIL-101. The FT-IR spectrum exhibits typical characteristics of both the samples, nanosized polyILs extracted from polyILs@MIL-101 and bulk polyILs, and the peaks around 1160 and 1040 $cm^{-1}$ are corresponding to the characteristic bands of imidazolium ring (Figure 1a).[38] Solid-



DOI: 10.1021/acscatal.7b03404
ACS Catal. 2018, 8, 3194−3201

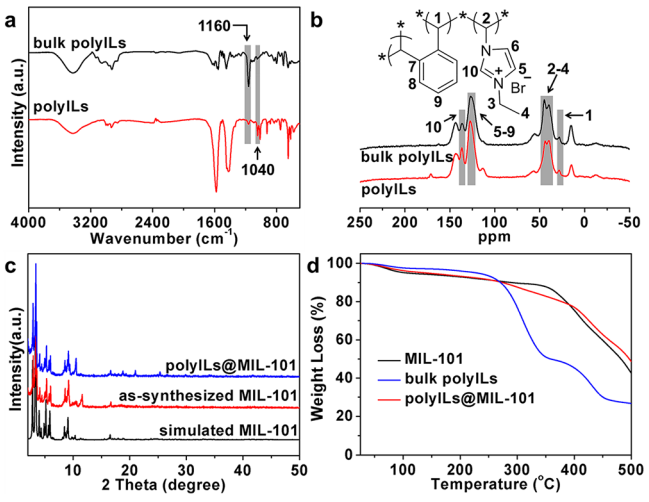


**Figure 1.** (a) FT-IR and (b) solid-state $^{13}C$ CP/MAS NMR spectra of bulk polyILs and polyILs obtained by removing the MOF from polyILs@MIL-101. (c) PXRD patterns of simulated and as-synthesized MIL-101 as well as polyILs@MIL-101 composite. (d) TG curves of MIL-101, bulk polyILs, and polyILs@MIL-101 in $N_2$ atmosphere.

state CP/MAS $^{13}C$ NMR spectra display similar peaks for both the samples, reflecting the covalent linking of two monomers. The chemical shift of the peak at 28 ppm is attributed to the C1 atom connected to the benzene ring, and the broad overlapping peaks at ~40 ppm are assigned to the C2−C4 atoms attached to the imidazolate ring (Figure 1b).[39] In addition, the resonance at ~126 ppm is ascribed to the C5 and C6 atoms of the imidazolate ring and the C7−C9 atoms in the benzene ring, whereas the peak at 136 ppm originates from the C10 atom of the imidazolate ring.[39] All of these signals confirm the nearly identical covalent binding of the two monomers in both samples and support the successful formation of proposed polyILs in MIL-101.

The powder XRD pattern of polyILs@MIL-101 shows sharp characteristic peaks indexed to MIL-101, demonstrating the crystallinity retention of MIL-101 after integration with polyILs (Figure 1c). Thermogravimetric (TG) analyses for MIL-101, bulk polyILs, and polyILs@MIL-101 show a similar weight loss before 100 °C, likely from the loss of low boiling point solvents (methanol and ethanol) in the samples (Figure 1d). In reference to MIL-101 decomposition at ~340 °C, the decomposition of bulk polyILs can be divided into two steps: the disintegration of the grafted ILs (the first step, 220−360 °C) and the collapse of the polymer matrix (the second step, 360−500 °C).[39] In the TG profile of the polyILs@MIL-101 composite, the observed weight losses around 260 and 390 °C might correspond to the removal of the grafted ILs and the mutual decomposition of MIL-101 and the polymer matrix, respectively. The higher decomposition temperatures of polyILs@MIL-101 indeed show higher thermal stability of the composites than that of the corresponding single components.

To verify the state of N and Br species in the composite, XPS was performed. The N 1s spectrum presents a peak at 401.0 eV, confirming the existence of positively charged nitrogen (—$N^+$=) of the imidazolium ring (Figure S2a).[35] Moreover, the high-resolution XPS spectrum for Br 3d reveals a weak peak at 68.4 eV, which is assigned to the negatively charged bromide ion (Figure S2b).[32,40,41] These results further prove that the monomers have been successfully incorporated into the composite.

The morphology and microstructure of bulk polyILs, MIL-101, and polyILs@MIL-101 were studied by scanning electron microscopy (SEM). Compared to the spongy morphology of bulk polyILs, polyILs@MIL-101 has an octahedral morphology similar to MIL-101, indicating that the formation of polyILs should be inside MIL-101 pores (Figures 2a,b and S3). To

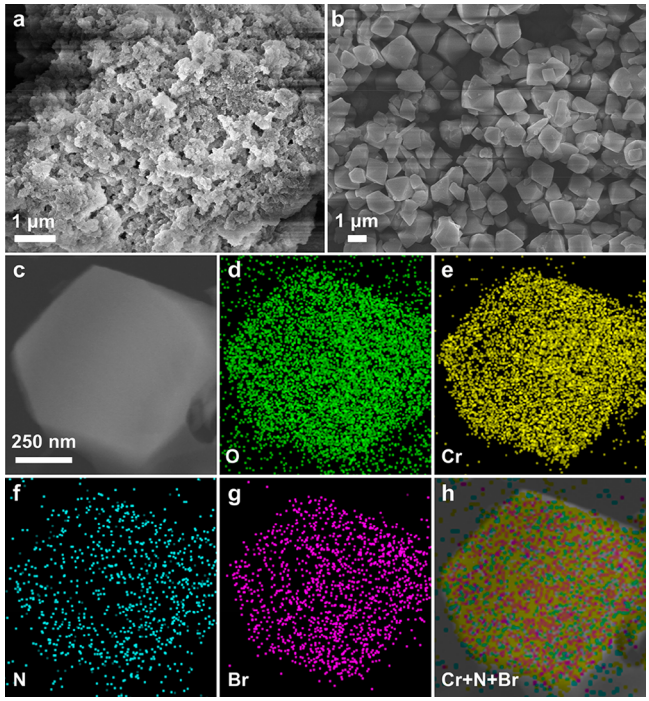


**Figure 2.** SEM images of (a) bulk polyILs and (b) polyILs@MIL-101. (c) TEM image of polyILs@MIL-101 particle slice and (d−h) corresponding elemental mapping of O, Cr, N, Br, and overlapping Cr + N + Br, respectively. The cross section of polyILs@MIL-101 is exposed after cutting the particle into slices.

further confirm that polymerization occurred inside the pores of MIL-101, the polyILs@MIL-101 particles were cut into slices for elemental mapping characterization. The TEM and elemental mapping results clearly show that all of the related elements, including N, Br, and C from polyILs and O, Cr, and C from MIL-101, are well distributed throughout the polyILs@MIL-101 slices (Figures 2c−h and S4), demonstrating that the copolymerization of monomers is mostly carried out in the cavities of MIL-101, instead of being coated on the MOF surface.

To evaluate the pore character, $N_2$ sorption was investigated for polyILs@MIL-101 at 77 K (Figure 3a). The Brunauer−Emmett−Teller (BET) surface area of 2462 $m^2/g$ and pore volume of 1.26 $cm^3/g$ for polyILs@MIL-101 are diminished compared to those of MIL-101 (3603 $m^2/g$ and 1.83 $cm^3/g$). The decreased surface area and pore volume of polyILs@MIL-101 are basically consistent with the increased weight from the polyILs. Compared with the parent MIL-101, the pore size distribution of polyILs@MIL-101 shows the shrinkage of pore size based on the density-functional theory (DFT) calculation, indicating that the cavities of MIL-101 are occupied by polyILs (Figure 3b). The hierarchical pores in polyILs@MIL-101 would facilitate the mass transport, and the reduced pore sizes might be actually beneficial for $CO_2$ capture.



DOI: 10.1021/acscatal.7b03404
ACS Catal. 2018, 8, 3194−3201

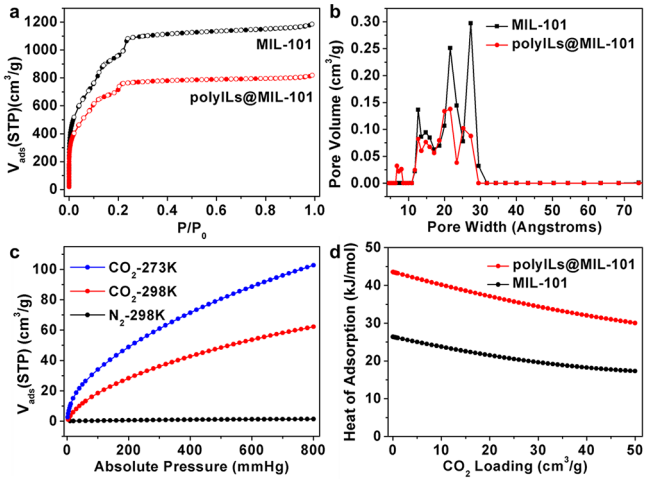


**Figure 3.** (a) $N_2$ sorption isotherms and (b) pore size distribution analyses based on the DFT method for MIL-101 and polyILs@MIL-101. (c) $CO_2$ and $N_2$ adsorption isotherms of polyILs@MIL-101 at different temperatures. (d) $CO_2$ isosteric heat of adsorption ($Q_{st}$) for MIL-101 and polyILs@MIL-101.

To validate this assumption, $CO_2$ sorption was measured for polyILs@MIL-101 and MIL-101 at 273 and 298 K (Figures 3c and S5). It was surprising that, compared to the $CO_2$ uptakes of MIL-101 (57 cm$^3$/g at 298 K and 89 cm$^3$/g at 273 K, 1 bar), the polyILs@MIL-101, even with a lower surface area of MIL-101, indeed exhibits higher $CO_2$ sorption capacities (62 cm$^3$/g at 298 K and 103 cm$^3$/g at 273 K, 1 bar), which should be attributed to the generation of additional small pores (<0.8 nm) upon loading polyILs.[42] In sharp contrast, polyILs@MIL-101 almost does not adsorb $N_2$ at 298 K (Figure 3c), despite its high $N_2$ sorption at 77 K and the large BET surface area (Figure 3a), showing a very high adsorption selectivity of $CO_2$/$N_2$. Additionally, the isosteric heat of $CO_2$ adsorption ($Q_{st}$) for polyILs@MIL-101, calculated by the virial method, clearly gives a higher value (44 kJ/mol) at zero coverage than that of MIL-101 (26 kJ/mol; Figure 3d), which shows the stronger affinity between $CO_2$ molecules and polyILs@MIL-101. Compared with MIL-101, the higher isosteric heat of adsorption of the polyILs@MIL-101 composite might be due to the confined pore size effect and the increase of aromatic surfaces.[43] After incorporating polyILs in the pores of MIL-101, the reduced pore size and increased surfaces would enhance the adsorbate–surface interactions between the composite and both sides or ends of the $CO_2$ molecules.[43] In addition, the IL-$CO_2$ interaction might also contribute to the improved $Q_{st}$ of polyILs@MIL-101.[44,45]

The interaction between $CO_2$ molecules and polyILs@MIL-101 was investigated by *in situ* DRIFT spectroscopy at room temperature. The background was measured with polyILs@MIL-101 (activated at 160 °C). Upon $CO_2$ adsorption, a strong peak at 2337 cm$^{-1}$ with a shoulder at 2325 cm$^{-1}$ was observed (Figure S6), which can be ascribed to the $\nu_3$ mode (asymmetric stretching mode) and the $\nu_3 + \nu_2 - \nu_2$ combination mode of $CO_2$, respectively.[46] The significant red shift of the $\nu_3$ mode of $CO_2$ compared with that of the gas phase (2349 cm$^{-1}$) originated from the H-bonds between $CO_2$ and the −OH groups of MIL-101, with very weak acidity.[46] Then, the $CO_2$ dosage was stopped and the DRIFT spectra were continually collected with Ar purging (Figure S6b-d). After Ar purging for 15 min, the intensities of the above two peaks were greatly reduced. In addition, several peaks assignable to the bicarbonate species, which originated from the interaction between $CO_2$ and −OH groups, were observed in the range of 1800–1300 cm$^{-1}$.[47] The intensities of these peaks were substantially unchanged even after Ar purging for 15 min, demonstrating the strong bonding between $CO_2$ and polyILs@MIL-101.

The acid property of polyILs@MIL-101 was examined by the temperature-programmed desorption (TPD) of ammonia ($NH_3$). Two broad peaks were observed in the range of 50–320 °C, validating the acidity in polyILs@MIL-101 (Figure S7).[48] The desorption peak in the low temperature range (50–210 °C) might be ascribed to the adsorption of $NH_3$ on the weak acid sites (i.e., Lewis $Cr^{3+}$ acid sites) of MIL-101, and the broad peak in the higher temperature range (210–320 °C) was possibly due to the partial decomposition of polyILs@MIL-101.[49,50] The Lewis acid concentration evaluated by the amount of desorbed $NH_3$ at relatively low temperature range is ~0.25 mmol/g.

With the confirmation of high surface area, good $CO_2$ sorption and interaction, the coexistence of the Lewis acid and Lewis base active sites, as well as the porous structure of polyILs@MIL-101 in hand, we set out to investigate its catalytic performance in the $CO_2$ cycloaddition with epoxides. To our delight, polyILs@MIL-101 possesses an excellent catalytic activity and achieves 94% yield toward the cycloaddition of epichlorohydrin to chloropropene carbonate with 1 bar $CO_2$ at 70 °C, in the absence of a cocatalyst (Figure 4a). Under similar

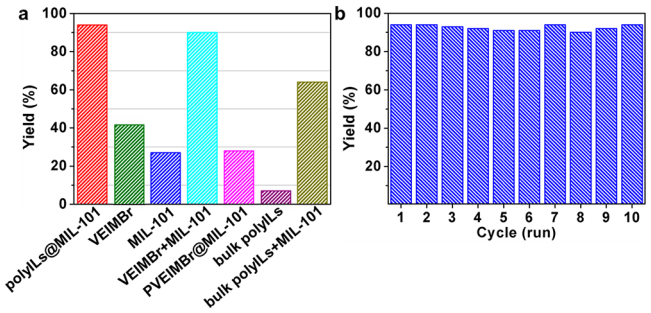


**Figure 4.** (a) Catalytic conversion of $CO_2$ cycloaddition with epichlorohydrin over different catalysts. (b) Recycling performance of polyILs@MIL-101 in ten consecutive runs of $CO_2$ cycloaddition.

conditions, VEIMBr and MIL-101 give only 42% and 27% conversion, respectively, which hints that both the Lewis base sites ($Br^-$ ions) from VEIMBr and the Lewis acid sites from MIL-101 work synergistically to enhance the catalytic activity. We also observed that a simple physical mixture of VEIMBr and MIL-101 converts 90% of the substrate into the target product, but the soluble VEIMBr in solvent is unfavorable for its separation and recycling from the reaction system. To check the necessity of the cross-linker o-DVB in the composite catalyst, the activity of PVEIMBr@MIL-101 synthesized by attempted polymerization of VEIMBr in MIL-101 was examined for the same reaction. Unexpectedly, PVEIMBr@MIL-101 gave an activity (28%) virtually similar to that of MIL-101 (27%), suggesting the unsuccessful polymerization of pure VEIMBr in the absence of the cross-linker o-DVB. Bulk polyILs and a physical mixture of bulk polyILs and MIL-101 were also employed in the control experiments, and they produced low conversions of 7% and 64%, respectively, under identical conditions, presumably owing to the very limited active sites available by bulk polyILs with low surface area (Figure S8). In


DOI: 10.1021/acscatal.7b03404
*ACS Catal.* 2018, 8, 3194–3201

sharp contrast, the active sites from polyILs would be much more accessible, thanks to the high surface area of polyILs@MIL-101. In addition, to study whether the change of hydrophobicity is associated with the catalytic activity,[51] the wettability of bulk polyILs, MIL-101 and polyILs@MIL-101 was evaluated by the water contact angle measurement. The contact angles (CA) of a water droplet on bulk polyILs, MIL-101, and polyILs@MIL-101 are ~14, ~31, and ~37°, respectively (Figure S9), showing that all of these catalysts are hydrophilic. There is no significant change of contact angle before and after incorporating polyILs into MIL-101. Therefore, the wettability in these catalysts might play negligible roles in their catalytic activities. The Lewis acid and Lewis base active sites (i.e., $Cr^{3+}$ ions of MIL-101 and $Br^-$ ions of ILs) are indeed the two important types of active sites in polyILs@MIL-101.

The recycling stability of a heterogeneous catalyst is of great importance for its practical application. Delightedly, the separation of polyILs@MIL-101 from the reaction mixture is readily realized by simple centrifugation, due to its heterogeneous nature. Remarkably, the catalytic activity of polyILs@MIL-101 is well retained during the 10 runs of the $CO_2$ cycloaddition reaction (Figure 4b). No significant loss of crystallinity and structural integrity for polyILs@MIL-101 was observed from the PXRD patterns after the reaction (Figure S10), suggesting excellent recyclability and stability of the composite catalyst.

Encouraged by the above outstanding catalytic performance of polyILs@MIL-101 in the $CO_2$ cycloaddition with epichlorohydrin, we also investigated the scope of this polyILs@MIL-101, catalyzing the $CO_2$ cycloaddition reaction with various epoxides (Table 1). Good to excellent conversions were achieved in almost all of the reactions, including terminal epoxides with both electron-withdrawing and electron-donating substituents (entries 1−6), indicating the great substrate tolerance of the composite catalyst for such a reaction. As an exception, the composite gave relatively low yield for cyclohexene oxide. A much higher reaction temperature (110 °C) and longer reaction time (72 h) are required to generate a 68% conversion yield, likely due to the significantly larger steric hindrance of cyclohexene oxide compared to other epoxides (entry 7).

**Table 1. $CO_2$ Cycloaddition with Epoxides Substituted with Different Functional Groups Catalyzed by polyILs@MIL-101**[a]

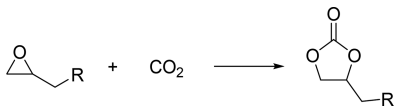


| Entry | Substrate | Temperature [°C] | Time [d] | Con.[b] [%] | Sel.[b] [%] |
|---|---|---|---|---|---|
| 1 |  | 45 | 2 | 94 | 100 |
| 2 | 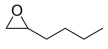 | 70 | 1 | 89 | 100 |
| 3 |  | 70 | 1 | 85 | 100 |
| 4 |  | 70 | 1 | >99 | 100 |
| 5 |  | 70 | 2 | 81 | 100 |
| 6 | 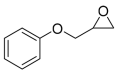 | 70 | 1 | 95 | 100 |
| 7[c] |  | 110 | 3 | 68 | 100 |

[a]Reaction conditions: 1 mmol of substrate, 100 mg of polyILs@MIL-101, 2 mL of acetonitrile, and 1 bar of $CO_2$. [b]Determined by gas chromatography. [c]2 mL of *N*,*N*-dimethylformamide.

To understand how the $CO_2$ uptake/enrichment capability of polyILs@MIL-101 contributes to its catalytic effect, the activities of polyILs@MIL-101 and VEIMBr, the main active component of the polyILs, have been investigated under different $CO_2$ pressures (Figure 5). Along with reduced $CO_2$ pressure from 1.5 to 0.5 bar, as expected, the catalytic activity of VEIMBr significantly decreases, owing to the diluted $CO_2$ concentration. In stark contrast, polyILs@MIL-101 exhibits no drop of catalytic activity at a $CO_2$ pressure ranging from 1.5 to 0.75 bar, and it retains decent activity (~80%) even under 0.5 bar of $CO_2$ pressure. These results can be explained by the fairly good $CO_2$ sorption in the pores of the composite catalyst (Figure 3c), greatly promoting $CO_2$ enrichment around the active sites and thus boosting its subsequent conversion. It is noteworthy that, although the positive correlation between $CO_2$ sorption and conversion was proposed previously,[14] the above catalytic $CO_2$ conversion efficiency at different $CO_2$ pressures (≤1.5 bar) over the polyILs@MIL-101 catalyst provides direct evidence for this correlation.

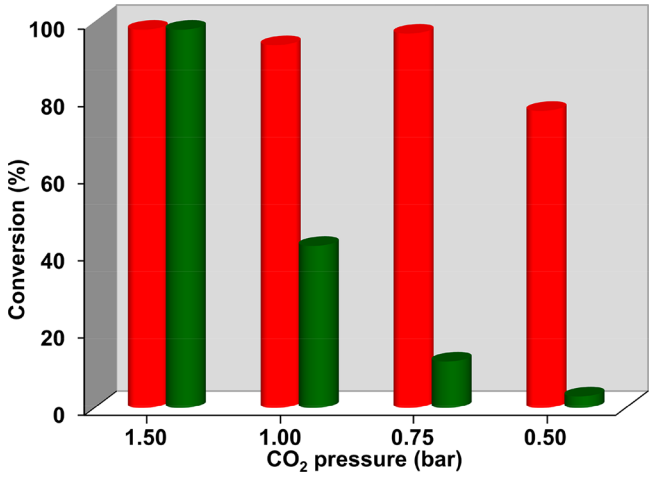


**Figure 5.** Catalytic conversion of $CO_2$ cycloaddition with epichlorohydrin over polyILs@MIL-101 (red column) and VEIMBr (olive green column) under different $CO_2$ pressures.

On the basis of the preceding results, a tentative mechanism for the $CO_2$ cycloaddition of epoxides to form cyclic carbonates can be proposed (Scheme S1). First, the epoxide is adsorbed and polarized by the coordinatively unsaturated Cr(III) sites (Lewis acid) in polyILs@MIL-101.[32] Subsequently, the ring-opening step occurs due to the nucleophilic attack of the bromide ion from polyILs on the less sterically hindered carbon atom of the epoxide. Then, the C atom of the $CO_2$ molecule is attacked by the ring-opened intermediate. Afterward, $CO_2$ inserts into the ring-opened intermediate to give an acyclic ester. Finally, the intramolecular cyclization of the acyclic ester results in the formation of cyclic carbonate, followed by the regeneration of the polyILs@MIL-101 catalyst.



DOI: 10.1021/acscatal.7b03404
ACS Catal. 2018, 8, 3194−3201

## 4. CONCLUSION

In summary, the imidazolium-based IL has been polymerized with *ortho*-divinylbenzene as the cross-linker inside MIL-101 pores to afford the bifunctional polyILs@MIL-101 composite, containing both Lewis acid and Lewis base active sites. Thanks to the high surface area, hierarchical pores, and synergistic effect between the two types of active sites, the resultant polyILs@MIL-101 composite possesses high activity toward $CO_2$ cycloaddition with epoxides, under mild conditions (1 bar $CO_2$, ≤70 °C), without the help of a cocatalyst. This composite also exhibits excellent recyclability and stability as a result of its heterogeneous nature and perfect incorporation of polyILs inside MIL-101. It is noteworthy that polyILs@MIL-101 is capable of enriching $CO_2$ at low partial pressure (0.5 bar) and still significantly retains its catalytic activity. This work not only provides a novel perspective to develop the IL-MOF composite catalyst, synergizing their respective strengths, but also directly demonstrates how the $CO_2$ uptake capability of the catalyst merits the $CO_2$ conversion.

## ■ ASSOCIATED CONTENT

### Supporting Information

The Supporting Information is available free of charge on the ACS Publications website at DOI: 10.1021/acscatal.7b03404.

Supplemental characterization results and mechanism figure. (PDF)

## ■ AUTHOR INFORMATION


### Corresponding Author

*E-mail: jianglab@ustc.edu.cn.

### ORCID

Hai-Long Jiang: 0000-0002-2975-7977


### Author Contributions

The manuscript was written through contributions of both authors. Both authors have given approval to the final version of the manuscript.

### Notes

The authors declare no competing financial interest.

## ■ ACKNOWLEDGMENTS

This work was supported by the National Research Fund for Fundamental Key Project (2014CB931803), the NSFC (21725101, 21673213, and 21521001), and the Recruitment Program of Global Youth Experts. We are grateful to the reviewers for their insightful comments and valuable suggestions and also thank Dr. Zhiyong U. Wang at Troy University for his fruitful discussion and manuscript refinement.

## ■ REFERENCES


(1) Zhang, Z.; Yao, Z.-Z.; Xiang, S.; Chen, B. Perspective of Microporous Metal-Organic Frameworks for $CO_2$ Capture and Separation. *Energy Environ. Sci.* **2014**, *7*, 2868−2899.

(2) Sanz-Pérez, E. S.; Murdock, C. R.; Didas, S. A.; Jones, C. W. Direct Capture of $CO_2$ from Ambient Air. *Chem. Rev.* **2016**, *116*, 11840−11876.

(3) Wang, W.; Wang, S.; Ma, X.; Gong, J. Recent Advances in Catalytic Hydrogenation of Carbon Dioxide. *Chem. Soc. Rev.* **2011**, *40*, 3703−3727.

(4) Trickett, C. A.; Helal, A.; Al-Maythalony, B. A.; Yamani, Z. H.; Cordova, K. E.; Yaghi, O. M. The Chemistry of Metal-Organic Frameworks for $CO_2$ Capture, Regeneration and Conversion. *Nature Rev. Mater.* **2017**, *2*, 17045.

(5) Maina, J. W.; Pozo-Gonzalo, C.; Kong, L.; Schütz, J.; Hill, M.; Dumée, L. F. Metal Organic Framework Based Catalysts for $CO_2$ Conversion. *Mater. Horiz.* **2017**, *4*, 345−361.

(6) Xu, H.-Q.; Hu, J.; Wang, D.; Li, Z.; Zhang, Q.; Luo, Y.; Yu, S.-H.; Jiang, H.-L. Visible-Light Photoreduction of $CO_2$ in a Metal-Organic Framework: Boosting Electron-Hole Separation via Electron Trap States. *J. Am. Chem. Soc.* **2015**, *137*, 13440−13443.

(7) He, H.; Perman, J. A.; Zhu, G.; Ma, S. Metal-Organic Frameworks for $CO_2$ Chemical Transformations. *Small* **2016**, *12*, 6309−6324.

(8) Decortes, A.; Castilla, A. M.; Kleij, A. W. Salen-Complex-Mediated Formation of Cyclic Carbonates by Cycloaddition of $CO_2$ to Epoxides. *Angew. Chem., Int. Ed.* **2010**, *49*, 9822−9837.

(9) Lu, X.-B.; Darensbourg, D. J. Cobalt Catalysts for the Coupling of $CO_2$ and Epoxides to Provide Polycarbonates and Cyclic Carbonates. *Chem. Soc. Rev.* **2012**, *41*, 1462−1484.

(10) Sneddon, G.; Greenaway, A.; Yiu, H. H. P. The Potential Applications of Nanoporous Materials for the Adsorption, Separation, and Catalytic Conversion of Carbon Dioxide. *Adv. Energy Mater.* **2014**, *4*, 1301873.

(11) Beyzavi, M. H.; Stephenson, C. J.; Liu, Y.; Karagiaridi, O.; Hupp, J. T.; Farha, O. K. Metal-Organic Framework-Based Catalysts: Chemical Fixation of $CO_2$ with Epoxides Leading to Cyclic Organic Carbonates. *Front. Energy Res.* **2015**, *2*, 63.

(12) Ding, M.; Chen, S.; Liu, X.-Q.; Sun, L.-B.; Lu, J.; Jiang, H.-L. Metal-Organic Framework-Templated Catalyst: Synergy in Multiple Sites for Catalytic $CO_2$ Fixation. *ChemSusChem* **2017**, *10*, 1898−1903.

(13) Wang, J.; Zhang, Y. Boronic Acids as Hydrogen Bond Donor Catalysts for Efficient Conversion of $CO_2$ into Organic Carbonate in Water. *ACS Catal.* **2016**, *6*, 4871−4876.

(14) Jiang, Z.-R.; Wang, H.; Hu, Y.; Lu, J.; Jiang, H.-L. Polar Group and Defect Engineering in a Metal-Organic Framework: Synergistic Promotion of Carbon Dioxide Sorption and Conversion. *ChemSusChem* **2015**, *8*, 878−885.

(15) Zhang, X.; Zhang, X.; Dong, H.; Zhao, Z.; Zhang, S.; Huang, Y. Carbon Capture with Ionic Liquids: Overview and Progress. *Energy Environ. Sci.* **2012**, *5*, 6668−6681.

(16) Zhao, Y.; Yao, C.; Chen, G.; Yuan, Q. Highly Efficient Synthesis of Cyclic Carbonate with $CO_2$ Catalyzed by Ionic Liquid in a Microreactor. *Green Chem.* **2013**, *15*, 446−452.

(17) Xu, B.-H.; Wang, J.-Q.; Sun, J.; Huang, Y.; Zhang, J.-P.; Zhang, X.-P.; Zhang, S.-J. Fixation of $CO_2$ into Cyclic Carbonates Catalyzed by Ionic Liquids: a Multi-Scale Approach. *Green Chem.* **2015**, *17*, 108−122.

(18) Wang, C.; Luo, H.; Luo, X.; Li, H.; Dai, S. Equimolar $CO_2$ Capture by Imidazolium-Based Ionic Liquids and Superbase Systems. *Green Chem.* **2010**, *12*, 2019−2023.

(19) Chen, W.; Zhang, Y.; Zhu, L.; Lan, J.; Xie, R.; You, J. A Concept of Supported Amino Acid Ionic Liquids and Their Application in Metal Scavenging and Heterogeneous Catalysis. *J. Am. Chem. Soc.* **2007**, *129*, 13879−13886.

(20) Han, L.; Park, S.-W.; Park, D.-W. Silica Grafted Imidazolium-Based Ionic Liquids: Efficient Heterogeneous Catalysts for Chemical Fixation of $CO_2$ to a Cyclic Carbonate. *Energy Environ. Sci.* **2009**, *2*, 1286−1292.

(21) Zheng, X.; Luo, S.; Zhang, L.; Cheng, J.-P. Magnetic Nanoparticle Supported Ionic Liquid Catalysts for $CO_2$ Cycloaddition Reactions. *Green Chem.* **2009**, *11*, 455−458.

(22) Xie, Y.; Zhang, Z.; Jiang, T.; He, J.; Han, B.; Wu, T.; Ding, K. $CO_2$ Cycloaddition Reactions Catalyzed by an Ionic Liquid Grafted onto a Highly Cross-Linked Polymer Matrix. *Angew. Chem., Int. Ed.* **2007**, *46*, 7255−7258.

(23) Wang, X.; Zhou, Y.; Guo, Z.; Chen, G.; Li, J.; Shi, Y.; Liu, Y.; Wang, J. Heterogeneous Conversion of $CO_2$ into Cyclic Carbonates at Ambient Pressure Catalyzed by Ionothermal-Derived Meso-Macroporous Hierarchical Poly(ionic liquid)s. *Chem. Sci.* **2015**, *6*, 6916−6924.

(24) Zhou, H.-C.; Kitagawa, S. Metal-Organic Frameworks (MOFs). *Chem. Soc. Rev.* **2014**, *43*, 5415−5418.




DOI: 10.1021/acscatal.7b03404
*ACS Catal.* 2018, 8, 3194−3201

(25) Li, J.-R.; Sculley, J.; Zhou, H.-C. Metal-Organic Frameworks for Separations. *Chem. Rev.* **2012**, *112*, 869−932.
(26) Islamoglu, T.; Goswami, S.; Li, Z.; Howarth, A. J.; Farha, O. K.; Hupp, J. T. Postsynthetic Tuning of Metal-Organic Frameworks for Targeted Applications. *Acc. Chem. Res.* **2017**, *50*, 805−813.
(27) Li, B.; Wen, H.-M.; Cui, Y.; Zhou, W.; Qian, G.; Chen, B. Emerging Multifunctional Metal-Organic Framework Materials. *Adv. Mater.* **2016**, *28*, 8819−8860.
(28) Fujie, K.; Kitagawa, H. Ionic Liquid Transported into Metal-Organic Frameworks. *Coord. Chem. Rev.* **2016**, *307*, 382−390.
(29) Parnham, E. R.; Morris, R. E. Ionothermal Synthesis of Zeolites, Metal-Organic Frameworks, and Inorganic-Organic Hybrids. *Acc. Chem. Res.* **2007**, *40*, 1005−1013.
(30) Luo, Q.; Ji, M.; Lu, M.; Hao, C.; Qiu, J.; Li, Y. Organic Electron-Rich N-Heterocyclic Compound as a Chemical Bridge: Building a Brönsted Acidic Ionic Liquid Confined in MIL-101 Nanocages. *J. Mater. Chem. A* **2013**, *1*, 6530−6534.
(31) Liang, J.; Chen, R.-P.; Wang, X.-Y.; Liu, T.-T.; Wang, X.-S.; Huang, Y.-B.; Cao, R. Postsynthetic Ionization of an Imidazole-Containing Metal-Organic Framework for the Cycloaddition of Carbon Dioxide and Epoxides. *Chem. Sci.* **2017**, *8*, 1570−1575.
(32) Ma, D.; Li, B.; Liu, K.; Zhang, X.; Zou, W.; Yang, Y.; Li, G.; Shi, Z.; Feng, S. Bifunctional MOF Heterogeneous Catalysts Based on the Synergy of Dual Functional Sites for Efficient Conversion of $CO_2$ under Mild and Co-catalyst Free Conditions. *J. Mater. Chem. A* **2015**, *3*, 23136−23142.
(33) Tharun, J.; Bhin, K.-M.; Roshan, R.; Kim, D. W.; Kathalikkattil, A. C.; Babu, R.; Ahn, H. Y.; Won, Y. S.; Park, D.-W. Ionic Liquid Tethered Post Functionalized ZIF-90 Framework for the Cyclo-addition of Propylene Oxide and $CO_2$. *Green Chem.* **2016**, *18*, 2479−2487.
(34) Ding, L.-G.; Yao, B.-J.; Jiang, W.-L.; Li, J.-T.; Fu, Q.-J.; Li, Y.-A.; Liu, Z.-H.; Ma, J.-P.; Dong, Y.-B. Bifunctional Imidazolium-Based Ionic Liquid Decorated UiO-67 Type MOF for Selective $CO_2$ Adsorption and Catalytic Property for $CO_2$ Cycloaddition with Epoxides. *Inorg. Chem.* **2017**, *56*, 2337−2344.
(35) Li, Z.; Wang, W.; Chen, Y.; Xiong, C.; He, G.; Cao, Y.; Wu, H.; Guiver, M. D.; Jiang, Z. Constructing Efficient Ion Nanochannels in Alkaline Anion Exchange Membranes by the *in situ* Assembly of a Poly(ionic liquid) in Metal-Organic Frameworks. *J. Mater. Chem. A* **2016**, *4*, 2340−2348.
(36) Marcilla, R.; Blazquez, J. A.; Rodriguez, J.; Pomposo, J. A.; Mecerreyes, D. Tuning the Solubility of Polymerized Ionic Liquids by Simple Anion-Exchange Reactions. *J. Polym. Sci., Part A: Polym. Chem.* **2004**, *42*, 208−212.
(37) Férey, G.; Mellot-Draznieks, C.; Serre, C.; Millange, F.; Dutour, J.; Surblé, S.; Margiolaki, I. A Chromium Terephthalate-Based Solid with Unusually Large Pore Volumes and Surface Area. *Science* **2005**, *309*, 2040−2042.
(38) Dai, W.-L.; Jin, B.; Luo, S.-L.; Yin, S.-F.; Luo, X.-B.; Au, C.-T. Cross-Linked Polymer Grafted with Functionalized Ionic Liquid as Reusable and Efficient Catalyst for the Cycloaddition of Carbon Dioxide to Epoxides. *J. CO2 Util.* **2013**, *3*−*4*, 7−13.
(39) Wang, X.; Li, J.; Chen, G.; Guo, Z.; Zhou, Y.; Wang, J. Hydrophobic Mesoporous Poly(ionic liquid)s towards Highly Efficient and Contamination-Resistant Solid-Base Catalysts. *ChemCatChem* **2015**, *7*, 993−1003.
(40) Silvester, D. S.; Broder, T. L.; Aldous, L.; Hardacre, C.; Crossley, A.; Compton, R. G. Using XPS to Determine Solute Solubility in Room Temperature Ionic Liquids. *Analyst* **2007**, *132*, 196−198.
(41) Kim, D.; Moon, Y.; Ji, D.; Kim, H.; Cho, D. Metal-Containing Ionic Liquids as Synergistic Catalysts for the Cycloaddition of $CO_2$: A Density Functional Theory and Response Surface Methodology Corroborated Study. *ACS Sustainable Chem. Eng.* **2016**, *4*, 4591−4600.
(42) Silvestre-Albero, J.; Rodríguez-Reinoso, F. Novel Carbon Materials for $CO_2$ Adsorption. *Novel Carbon Adsorbents*; Elsevier: London, 2012; pp 583−603.
(43) Ding, N.; Li, H.; Feng, X.; Wang, Q.; Wang, S.; Ma, L.; Zhou, J.; Wang, B. Partitioning MOF-5 into Confined and Hydrophobic Compartments for Carbon Capture under Humid Conditions. *J. Am. Chem. Soc.* **2016**, *138*, 10100−10103.
(44) Izgorodina, E. I.; Hodgson, J. L.; Weis, D. C.; Pas, S. J.; MacFarlane, D. R. Physical Absorption of $CO_2$ in Protic and Aprotic Ionic Liquids: An Interaction Perspective. *J. Phys. Chem. B* **2015**, *119*, 11748−11759.
(45) Park, Y.; Lin, K.-Y. A.; Park, A.-H. A.; Petit, C. Recent Advances in Anhydrous Solvents for $CO_2$ Capture: Ionic Liquids, Switchable Solvents, and Nanoparticle Organic Hybrid Materials. *Front. Energy Res.* **2015**, *3*, 42.
(46) Vimont, A.; Travert, A.; Bazin, P.; Lavalley, J.-C.; Daturi, M.; Serre, C.; Férey, G.; Bourrelly, S.; Llewellyn, P. L. Evidence of $CO_2$ Molecule Acting as an Electron Acceptor on a Nanoporous Metal-Organic-Framework MIL-53 or $Cr^{3+}(OH)(O_2C\text{-}C_6H_4\text{-}CO_2)$. *Chem. Commun.* **2007**, 3291−3293.
(47) Ferretto, L.; Glisenti, A. Surface Acidity and Basicity of a Rutile Powder. *Chem. Mater.* **2003**, *15*, 1181−1188.
(48) Kim, J.; Kim, S.-N.; Jang, H.-G.; Seo, G.; Ahn, W.-S. $CO_2$ Cycloaddition of Styrene Oxide over MOF Catalysts. *Appl. Catal., A* **2013**, *453*, 175−180.
(49) Pan, Y.; Yuan, B.; Li, Y.; He, D. Multifunctional Catalysis by Pd@MIL-101: One-Step Synthesis of Methyl Isobutyl Ketone over Palladium Nanoparticles Deposited on a Metal-Organic Framework. *Chem. Commun.* **2010**, *46*, 2280−2282.
(50) Chen, Y.-Z.; Zhou, Y.-X.; Wang, H.; Lu, J.; Uchida, T.; Xu, Q.; Yu, S.-H.; Jiang, H.-L. Multifunctional PdAg@MIL-101 for One-Pot Cascade Reactions: Combination of Host-Guest Cooperation and Bimetallic Synergy in Catalysis. *ACS Catal.* **2015**, *5*, 2062−2069.
(51) Liu, F.; Huang, K.; Zheng, A.; Xiao, F.-S.; Dai, S. Hydrophobic Solid Acids and Their Catalytic Applications in Green and Sustainable Chemistry. *ACS Catal.* **2018**, *8*, 372−391.


DOI: 10.1021/acscatal.7b03404
*ACS Catal.* 2018, 8, 3194−3201